Available online at www.sciencedirect.com
SCIENCE DIRECT
Journal of Photochemistry and Photobiology A: Chemistry 181 (2006) 1–11
Journal of Photochemistry and Photobiology A:Chemistry
www.elsevier.com/locate/jphotochem

Two-photon polymerisation for three-dimensional micro-fabrication

Shuhui Wu *, Jesper Serbin, Min Gu *

Centre for Micro-Photonics and Centre for Ultrahigh-Bandwidth Devices for Optical Systems (CUDOS), Faculty of Engineering and Industrial Sciences, Swinburne University of Technology, PO Box 218, Hawthorn, Vic. 3122, Australia

Received 15 November 2005; received in revised form 2 March 2006; accepted 4 March 2006
Available online 18 April 2006

Abstract

This article presents an overview of the recent work related to the fabrication of three-dimensional (3D) micro-structures and photonic devices by means of the two-photon polymerisation (2PP) technology. The principle of the 2PP technique and the method for micro-fabrication are introduced in this article. The solidified size of a micro-structure formed during the photo-polymerisation process can be controlled by adjusting optical fabrication parameters; the minimum size can be as small as 150 nm. The influence of photo-initiators and material properties of a resin are discussed. Recent progress related to the development of initiators and resins for 2PP is briefly introduced. Chemical processes, preparation procedures and post-processing of the common resins (including commercialised and customer-made ones) are summarised in tables. Micro-structures such as photonic crystal woodpile structures fabricated by using various resins are reviewed. The performance indicators of common resins for photonic crystal application are emphasised.

Keywords: Photosensitive resin; Two-photon polymerisation; Three-dimensional micro-fabrication

1. Introduction

Two-photon polymerisation (2PP) is a powerful technology which has recently been applied to generate three-dimensional (3D) micro-structures. This new application has drawn great attention because of the following reasons: (1) it can generate any kind of 3D structures based on computer generated 3D models; (2) the fabrication procedure is simple and fast; (3) the resolution of the structures can be as small as 150 nm; (4) the fabricated structures can be integrated into complicated devices. Although there has been rapid progress in the development of this technology, there is no systemic review to summarise the recent developments in this area. In this paper, we will introduce the historic background and recent development of the 2PP technology for 3D micro-fabrication, as well as our recent research work on this topic. Section 2 introduces the historic background of the two-photon technology, and its application in 3D micro-fabrication. In Section 3, we discuss the theoretical limitation of resolution of process. Section 4 focuses on the influence of photo-initiators (PI) including commercial ultraviolet (UV) initiators and special two-photon initiators. Section 5 covers a range of polymer materials for the fabrication as well as some examples of micro-structures generated by means of 2PP. The performance of different polymer resins for photonic crystal applications is emphasised.

2. Fundamental of two-photon polymerisation

2.1. Two-photon absorption

Two-photon absorption (2PA) is a radiation–matter interaction that consists in the excitation of an atom or a molecule from a lower quantum state |1> to an excited state |2> of the same parity as |1> in a single step [1]. In contrast to single-photon absorption, this transition thus cannot be described as a dipole transition. The theory of 2PA was first developed by Maria Göppert-Mayer in 1931 in her PhD thesis [2]. As a two-

Abbreviations: CAD, computer aided design; CCD, charge-coupled device; 3D, three-dimensional; fs, femosecond; fcc, face-centered-cubic; IR, infrared; NA, numerical aperture; ND, neutral density filter; NIR, near-infrared; OPO, optical parametric oscillator; PI, photo initiator; 2PA, two-photon absorption; 1PP, single-photon polymerisation; 2PP, two-photon polymerisation; UV, ultraviolet

* Corresponding authors at: Centre for Micro-Photonics, Faculty of Engineering and Industrial Sciences, Mail 38, Swinburne University of Technology, PO Box 218, Hawthorn, Vic. 3122, Australia. Tel.: +61 3 9214 4314/8776; fax: +61 3 9214 5435.
E-mail addresses: swu@swin.edu.au (S. Wu), mgu@swin.edu.au (M. Gu).

1010-6030/$ – see front matter © 2006 Elsevier B.V. All rights reserved.
doi:10.1016/j.jphotochem.2006.03.004

Nomenclature

List of symbols

A	electron acceptor
c	unit heights pf woodpile structure ($c = 2\delta z$)
C	C is defined as the equation – $C = \ln[\rho_0(\rho_0 - \rho_{th})]$ (Section 3)
d	pixel diameter
D	electron donor
h	height of one-dimensional rods (in woodpile structure) with ellipse cross-section
l	pixel length
n	the number of pulses
$N = N(r, z, t)$	photon flux
N_0	constant of photon flux
P	the average laser power
r	distance to the optical axis (cylindrical coordinates)
r_0	focal diameter
$R^{\bullet}$, R^+	free radical and reactive cations
t	the total processing-irradiation time
w	width of one-dimensional rods (in woodpile structure) with ellipse cross-section
z	distance to the focal plane (cylindrical coordinates)
z_R	the Rayleigh length

Greek letters

δx	in-plane distance of woodpile structure
δz	layers spacing of woodpile structure ($\delta z = c/4$)
η	efficiency of the initiation process (<1)
λ	light wavelength
ν	the laser-pulse repetition rate
ρ	particle density of radicals
ρ_0	the primary initiator particle density
ρ_{th}	certain minimum density of radicals to allow polymerisation happening (threshold value)
σ_2	effective two-photon cross section for the generation of radicals
σ_2^a	ordinary two-photon absorption cross section
τ_L	the laser-pulse duration
ϕ_H^+	quantum yield for photo-generated acid value
φ	the fraction of light transmitted through the objective
ω	an normalized frequency
ω_L	frequency of the laser light

photon process, 2PA is closely related to Raman scattering, both of them are third order optically non-linear processes and involve the interaction of a medium with two photons without any excited intermediate state (of resonance). Much high intensities are needed for 2PA since two photons have to be absorbed simultaneously, where for Raman scattering only one photon is absorbed and another simultaneously emitted. Here, the energy difference of the two photons is retained by the molecule. While spontaneous Raman scattering was first observed in 1928 [3], 2PA could not be observed until 1961 [4], when the laser was invented. The reason for that is the fact that Raman scattering is proportional to the intensity of the incident light while 2PA is proportional to the square of the light intensity. Thus to observe 2PA, a laser is needed to provide the high intensity. 2PA is an important tool in laser spectroscopy since transitions between two states that cannot be connected by dipole transitions can be observed. One of the most common applications of 2PA is two-photon confocal microscopy [5] where the fluorescence of a dye molecule is observed after being excited by means of 2PA. The latter application also benefits from the fact that 2PA can be initialised anywhere in the volume of a transparent medium, see Fig. 1(a) and (b) (Fig. 1(a) shows a single-photon excited fluorescence, light is scattered; Fig. 1(b) is in two-photon situation, the fluorescence is confined to the focal volume) [6], and from the high resolution that can be achieved when working with two-photon excited spots. Using standard immersion oil objective lenses with a numerical aperture of NA = 1.4, a lateral resolution in order of 100 nm and an axial resolution of 500 nm can be achieved [7]. 2PA is the fundamental process making two-photon polymerisation possible which will be introduced in Section 2.2.

2.2. Two-photon polymerisation

A normal single-photon polymerisation (1PP) process consists of the following steps:

$$h\nu_{UV} + \text{initiator} \rightarrow R^{\bullet} \text{ or } R^+$$
$$R^{\bullet} \text{ or } R^+ + \text{monomers}$$
$$\rightarrow \text{free radical or cationic polymerisation} \quad (2.1)$$

In a 1PP process, an initiator only absorbs one UV photon with a short wavelength through linear absorption. There are a lot of well-known applications for 1PP like UV-photolithography or stereolithography, where a single UV photon is needed to initiate the polymerisation process near the surface of a photosensitive resin as shown in Fig. 2(a). Depending on the concentration of PI of optionally added absorber molecules, the UV light is absorbed by the resin within the first few micrometers. Thus, 1PP is a planar process restricted to the surface of the resin.

For a 2PP process, the first step of the reaction is different to 1PP process:

$$2h\nu_{NIR} + \text{initiator} \rightarrow R^{\bullet} \text{ or } R^+ \quad (2.2)$$

In a 2PP process, an initiator absorbs two near infrared (NIR) photons with a long wavelength through non-linear absorption. Two NIR photons are absorbed simultaneously by a PI molecule. Since the cross section for 2PA is orders of magnitude lower than for single photon absorption, the excitation beam intensities should be in order of TW/cm^2 to generate a sufficiently high density of radicalised starter molecules, especially when using PIs that are not optimised with respect to high 2PA cross-section. For NIR light, the used photosensitive resins are transparent,

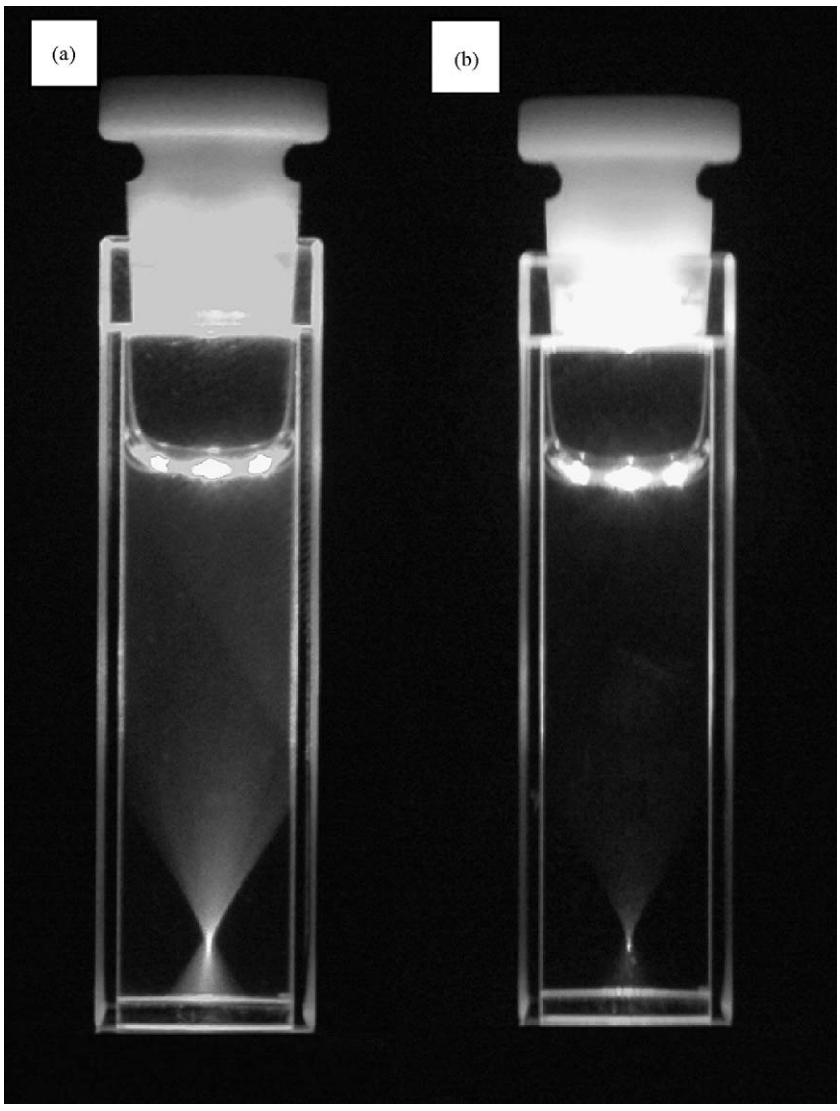

Fig. 1. (a) A fluorescent dye is excited with UV light. Most of the light is absorbed as the light enters the sample and fluorescence can be seen everywhere along the path of the light. (b) A fluorescent dye is excited with NIR ultrashort laser pulses. Due to the non-linear light-matter-interaction the excited spot is confined to the focal volume of the laser light.

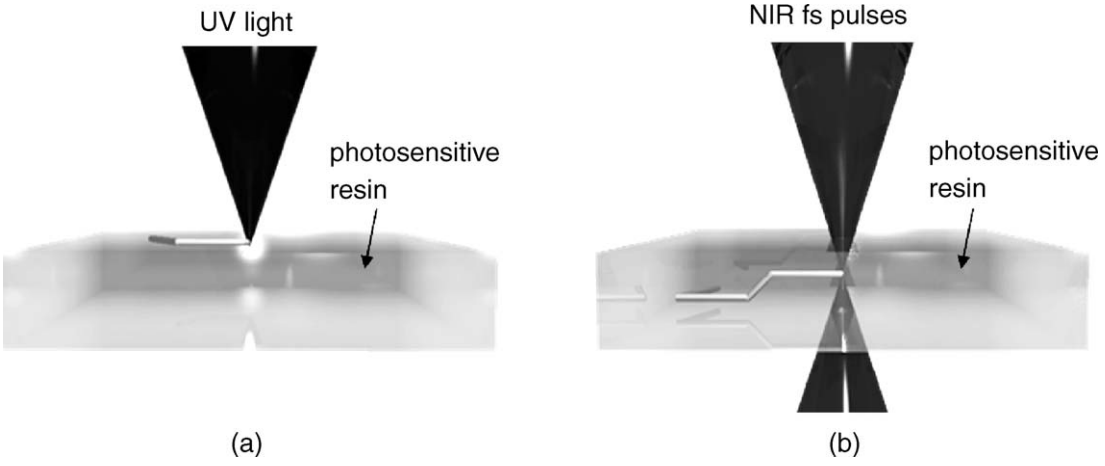

Fig. 2. (a) UV light is absorbed at the surface of a photosensitive polymer and can only be used for fabrication of planar structures (1PP). (b) NIR light can be focused into the volume of the UV-sensitive resin and can therefore be used for truly 3D structuring (2PP).

i.e. NIR femosecond (fs) laser pulses can be focused into the volume of the resin. If the photon density exceeds a certain threshold value, two-photon absorption occurs within the focal volume initiating the polymerisation process. When the laser focus is moved three-dimensionally through the volume of the resin, the polymerisation process is initiated along the trace of the focus allowing the fabrication of any 3D micro-structure, as illustrated in Fig. 2(b). The 3D movement of the laser focus can either be realised by scanning the laser in the x–y-plane using a galvo-scanner while moving the sample in the z-direction or by moving the sample three-dimensionally using a 3D piezo stage. Obviously, there are several advantages of 2PP compared to 1PP:

First, since the polymerisation can be initiated within the volume of the resin rather than being restricted to the surface, 2PP is a true 3D process whereas 1PP is a planar process. Applying 1PP, 3D structures can only be fabricated by means of working 2.5-dimensionally, i.e. working layer-by-layer. However, this limits the resolution (as in stereolithography, where the smallest achieved structure sizes are several micrometers) and does not allow for a rapid single step fabrication process.

Second, photo-polymerisation in contact with oxygen leads to quenching of the radicalised molecules on the surface of the resin and hence to a suppression of the polymerisation process. Therefore, high resolution 1PP processes have to be performed in an inert gas atmosphere. This drawback can be overcome by working in the volume rather than at the surface as it is done in 2PP.

Third, the two-photon excited spot is smaller than a single-photon excited spot, allowing the fabrication of smaller structures with resolution down to the submicron-size as explained in Section 3.

However, since the 2PP process is a direct laser-writing method, it is a serial process and imaging techniques for large structure fabrication cannot be applied as in UV-lithography.

For the principle described in this section, the 2PP technology can be applied to do 3D fabrication of micro-structures in polymer materials [8–20]. This method can replace the traditional optical devices fabrication method by means of lithography and etching processes as on silicon substrates, which include many complicated and time-consuming steps [21], the corresponding fabrication process can be simplified into the single-step generation of 3D structures by laser-induced photo-polymerisation. The 2PP method can produce the micro-structure replicate to the light pattern.

Due to the high radical density requirement of the 2PP process, a fs-pulsed laser is needed to combine with high numerical aperture (NA) focusing to provide a high light intensity spot. Fig. 3 is a typical fabrication set-up to generate micro-structures [13]. NIR fs laser pulses generated in a Ti:Sapphire laser are converted to the visible by means of an optical parametric oscillator (OPO). A neutral density filter (ND) is introduced into the beam path allowing for adjustments in beam intensity. The telescope arrangement leads to uniform illumination over the backaperture of an oil immersion objective. The beam is focused into a sample to initiate polymerisation. The sample, a photo-sensitive liquid resin, is sandwiched between two coverslips and mounted at a 3D piezoelectric scanning stage. The movement of the scanning

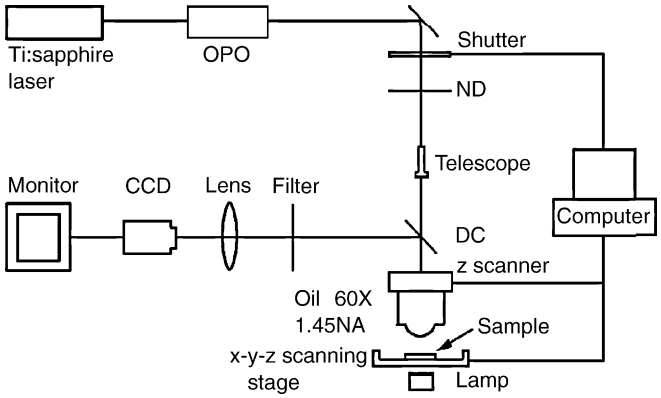

Fig. 3. Experimental setup for 3D microfabrication by means of 2PP.

stage is pre-programmed to form different micro-structures and controlled by a computer. The fabrication process is monitored by a charge-coupled device (CCD) camera. The requirements for photo-sensitive resin are discussed in Section 5.

3. Resolution of a 2PP process

Due to the threshold behaviour of the 2PP process, resolution beyond the diffraction limit can be realised by control of the laser-pulse energy and the number of applied pulses (see Fig. 4). To predict the size of the polymerised volume (or volume pixel or voxel) one first needs to define a polymerisation threshold. We assume that the resin is polymerised as soon as the particle density of radicals, $\rho = \rho(r, z, t)$, exceeds a certain minimum concentration (threshold value) ρ_{th} [18]. Due to the rotational symmetry of the intensity distribution, ρ can be treated as a function of z (distance to the focal plane in cylindrical coordinates) and r (distance to the optical axis in cylindrical coordinates), and here t is the total processing-irradiation time. For the same initiator, ρ_{th} is independent of the particular initiation process that leads to the generation of

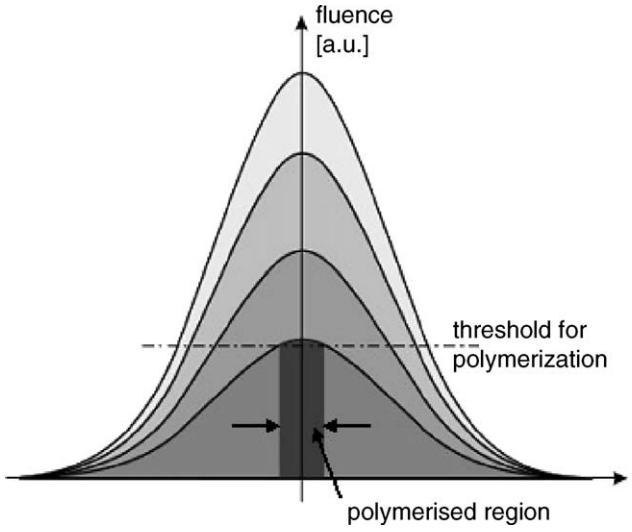

Fig. 4. Distribution of light in the laser focus. The well defined polymerisation threshold allows the generation of structures below the diffraction limit if working with laser powers just slightly above the threshold.

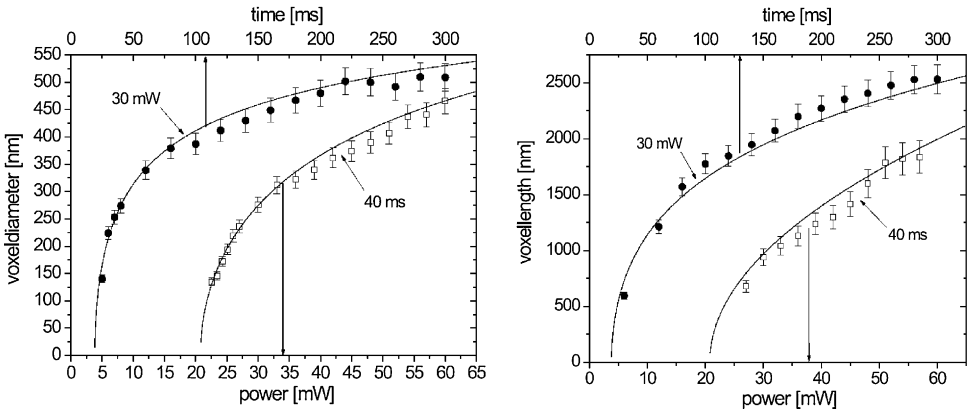

Fig. 5. Measured and estimated voxel sizes (length and diameter) as a function of time and laser power for Ormocer resin.

radicals and should be the same for single- and two-photon absorption.

The density of radicals, $\rho(r, z, t)$, produced by fs laser pulses can be calculated by solving a simple rate equation [18]:

$$\frac{\partial \rho}{\partial t} = (\rho_0 - \rho)\sigma_2 N^2, \tag{3.1}$$

where

$$\sigma_2 = \sigma_2^{\mathrm{a}}\eta. \tag{3.2}$$

Here σ_2 is the effective two-photon cross section for the generation of radicals, σ_2^{a} the ordinary two-photon absorption cross section, and η (<1) is the efficiency of the initiation process. $N = N(r, z, t)$ is the photon flux, ρ_0 is the primary initiator particle density. We can approximate the light distribution in the main maximum at the focal plane ($z = 0$) by a Gaussian distribution which is given by:

$$N(r, t) = N_0(t) \exp\left(\frac{-2r^2}{r_0^2}\right). \tag{3.3}$$

The photon flux on the optical axis, $N_0(t) = N_0$, is considered to be constant during the laser pulse, since reaching the polymerisation threshold requires many laser pulses. Neglecting the losses of radicals between the laser pulses, one obtains the following estimation for the pixel diameter (d), defined as a region where $\rho(r, z) \geq \rho_{\mathrm{th}}$ is fulfilled:

$$d(N_0, t) = r_0 \left[\ln\left(\frac{\sigma_2 N_0^2 n \tau_{\mathrm{L}}}{C}\right)\right]^{1/2}, \tag{3.4}$$

where $n = \nu t$ is the number of pulses, ν the laser-pulse repetition rate, t the total processing-irradiation time, and τ_{L} is the laser-pulse duration. Here C is defined as follow equation:

$$C = \ln[\rho_0(\rho_0 - \rho_{\mathrm{th}})]. \tag{3.5}$$

To estimate the maximum voxel length along the beam axis at $r = 0$, one can use the expression for the axial light distribution, $N(z) = N_0/(1 + z^2/z_{\mathrm{R}}^2)$, as for a Gaussian laser pulse. In this approximation, the pixel length l is determined by:

$$l(N_0, t) = 2z_{\mathrm{R}} \left[\left(\frac{\sigma_2 N_0^2 n \tau_{\mathrm{L}}}{C}\right)^{1/2} - 1\right]^{1/2}, \tag{3.6}$$

where z_{R} is the Rayleigh length.

By using Eqs. (3.4) and (3.6) the diameter and length of a polymerised voxel can be predicted. Fig. 5 is the comparison of predicted and measured data (left – diameter, right – length), where the value N_0 is replaced by:

$$N_0 = \frac{2}{\pi r_0^2 \tau_{\mathrm{L}}} \frac{P\varphi}{\nu \hbar \omega_{\mathrm{L}}}. \tag{3.7}$$

Here P is the average laser power, φ the fraction of light transmitted through the objective, and ω_{L} is frequency of the laser light. The measured data is mostly identical to the estimated value [18].

4. Influence of initiators

4.1. Commercial photo-initiators

Commercialised PI for UV curing systems can absorb photons from the incident radiation. Light absorption by the PI requires that the emission line from the light source overlaps with an absorption band of the PI. The energy of the photon is transferred to electronic structure of the PI molecule, and PI can convert this light energy into chemical energy in the form of reactive intermediates, such as free radicals ($R^{\bullet}$) or reactive cations (R^{+}), which subsequently initiate polymerisation of the monomers and oligomers [22], The process is shown in reaction (2.1).

Upon exposure to the UV light or two-photon of NIR light, the PI is photolysised to produce free radicals via molecular bond cleavage. The bond must have a dissociation energy lower than the excitation energy of the reactive excited state. Fig. 6 shows the various pathways of deactivation and activation for an excited commercial initiator. After absorbing energy from UV light or two-photon of NIR light, an initiator transfers from ground state to excited singlet or triplet state, part of the absorbed energy

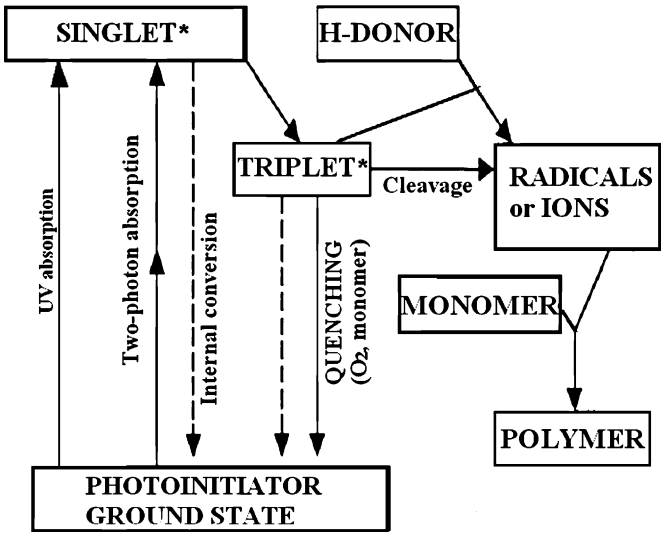

Fig. 6. Various pathways for deactivation and activation of the excited commercial initiator.

may be lost due to internal conversion from excited state to ground state, and some reactive intermediates can be quenched by oxygen, monomer (inefficient energy or electron transfer) and recombination of intermediates. Some of the excited initiators can abstract hydrogen from hydrogen donor and undergo a photo-induced electron transfer and fragmentation process to produce efficient reactive intermediates. Hydrogen abstraction is a typical reaction of triplet excited diarylketones. The triplet energy is high enough to overcome the bond energy of a carbon hydrogen bond which make it be broken from an activated position (α or β cleavage). The reactive intermediates interact with monomer and trig polymerisation chain reaction. Other initiators may undergo directly a fragmentation process without abstracting hydrogen from donors [17,22].

The polymerisation rate depends on the light source intensity, the PI concentration, the presence of oxygen and additives, the quantum yield of the radical generation and the initiation efficiency of generated radicals. Generally, the rate is increased with the incident light intensity, but not with initiator concentration. If an initiator has high extinction coefficient, high concentration of initiators can led to inefficient energy transfer. Different concentrations of initiators can also led to different molecular weight and molecular weight distributions, resulting in final polymer with various mechanical properties. Therefore, the concentrations of initiators should be chosen carefully to obtain the optimised performance of a micro-structure. An ideal initiator should have high molar absorption coefficients, a low extinction efficient and a well-adapted spectral absorption range. It can produce intermediate with excellent reactivity and photolysis by-products with low toxicity. Further it should be compatible with monomer and oligomers, dispersing in the monomer uniformly before photo-polymerisation.

In a 2PP system, a resin containing commercial UV initiator can be used to fabricate micro-devices according to the principle described in Sections 2 and 3. For a specific initiator, the maximum absorption wavelength prefers to be as half as the wavelength of the fabrication beam. If an initiator of absorption above a certain level is ranged from λ_1 to λ_2, the fabrication wavelength should be ranged between $2\lambda_1$ and $2\lambda_2$. Fabrication parameters like the intensity of light, the wavelength of the beam, the exposure time and the scanning speed are also needed to be chosen carefully in order to obtain an optimised micro-structure corresponding to the designed requirement.

In Table 1 some commercialised UV initiators from Ciba Specialty Chemicals are listed. These initiators may also be available in other chemical suppliers, CAS number provided here is the universal reference number for the same chemical product.

4.2. Two-photon initiator

Because the two-photon technology has great potential application in the area of 3D fluorescence microscopy, 3D microfabrication and optical data storage areas, it is important to design and synthesis of highly active organic two-photon chromophores. Up to now, fully understanding the relationship of the molecular structure and property with varied structural parameters and precisely reproducing characterisation of two-photon properties still remains a big challenge for researchers. But the major design concept is based on the relationship between the molecular two-photon cross-section and the imaginary components of the third-order non-linear susceptibility [23–25].

A typical structure of the two-photon initiator is the π-conjugation bridge chromophore with high planarity substitudes of electron donor (D) or electron acceptor (A). Type I structure is symmetrical, such as D–π–D, D–π–A–π–D, A–π–D–π–A molecules. Type II the molecular is asymmetrical, like D–π–A molecules. There are a series of strategies to increase the cross-section of molecules [24,25]:

(1) Extending the π-conjugation length.
(2) Increasing the planarity of the chromophore by using fused aromatic rings π-bridge.
(3) Increasing the strength of donors and acceptors.

Table 1
Some commercialised UV initiators supplied by Ciba Specialty Chemicals

Trade name	Chemical name	CAS number	Molecular weight
IRGACURE® 369	2-Benzyl-2-dimethylamino-1-(4-morpholinophenyl)-butanone-1	119313-12-1	366.5
IRGACURE® 184	1-Hydroxy-cyclohexyl-phenyl-ketone	947-19-3	204.3
IRGACURE® 819	Bis(2,4,6-trimethylbenzoyl)-phenylphosphineoxide	162881-26-7	418.5
DAROCUR® 1173	2-Hydroxy-2-methylpropiophenone	7473-98-5	164.3
IRGACURE® 1000	(80% DAEOCUR® 1173; 20% IRGACUER® 184)	–	–

For a normal UV initiator, the two-photon cross-section is very small ($<10 \times 10^{-50}$ cm^4 second per photon). By using the molecule with above-mentioned structures, the two-photon cross-section can be increased in order of 1000×10^{-50} cm^4 second per photon [26,27].

For an initiator, the molecules should not only have the large two-photon absorption cross-section, but also should have high efficiency to produce reactive intermediate radicals or cations, just like normal UV initiators. The intermediates can efficiently activate the chemical functionality. Upon using the two-photon initiator, the photo-sensitivity of whole system is increased. It can lower the polymerisation threshold; therefore the laser-writing window can become broader, and the possibility to damage the structure due to the high fabrication intensity and the long exposure time associated with commercial UV initiators can be reduced. In some cases, two-photon initiators can increase the polymerisation rate.

The methods used to characterise the two-photon activity are non-linear transmission, up-converted fluorescence emission, transient absorption, four-wave mixing and *Z*-scan technique, etc. [25]. These technologies can be used to measured the cross-section of a molecule and the quantum yield of an initiator. Zhou et al. synthesised a two-photon-generated photo-acid which can be applied to initiate cationic polymerisation, with cross-section as 690×10^{-50} cm^4 second per photon and high quantum yield for photo-generated acid value of $\varphi_H^+ = 0.5$ [26]; Cumpston synthesised an initiator for radical polymerisation with cross-section ranged $200–1200 \times 10^{-50}$ cm^4 second per photon, greatly increasing the fluorescent image contrast and the photo-sensitivity of fabrication system [27]. Currently the developed two-photon initiators are only applied in science laboratory for fundamental research use.

5. Materials and devices

5.1. Materials

Polymer materials are chosen for micro-fabrication because polymers are inexpensive, easy to process and able to be fabricated simply. Polymer materials are also flexible to be modified into composites to achieve chemical and physical functionality. Resins used to fabricate micro-structures are multi-functional monomers or oligomers. A PI is chosen to be added into a resin through solvent-mixing process. A pulsed laser beam excites the initiator to produce radicals or cations, then they interact with the surrounding monomers to trigger a polymerisation chain reaction as shown in reactions (2.1) or (2.2). Multi-functional monomers can form a crosslinked network within the focal volume of the laser beam, which cannot be dissolved by any solvent. The resin is solidified by the two-photon excitation beam through the pre-programmed light pathway to form a 3D micro-structure. The non-crosslinked monomers maintain good solubility in certain solvents and can be washed away after the 2PP process, leaving a 3D micro-structure which is an exact replicate to the pathway of the laser focus.

Resins used for fabrication must be transparent in the visible and NIR region to allow for focusing the laser pulses into the volume of the resin without any single-photon interaction. They should have a fast curing speed and the polymerised area should be confined to the focal spot with only little scattering. The highly crosslinked material must have washout resistance and should not swell or be deformed by any solvent; therefore the fabricated micro-structure remains unharmed upon the development process. Photosensitive resins generally show shrinking behaviour during the polymerisation process, the shrinkage and resulted distortion to the structure should be kept as small as possible. The refractive index of the resin before fabrication should be close to that of glass which is approx. 1.5; this allows the beam to be focused deeply into the resin without aberrations to access a large vertical dimension. After polymerisation, the refractive index generally changes to a slightly higher value, which increases the contrast in refractive indices between the polymer and air. This behaviour enhances the performance of photonic crystal structures. The thermal stability of the crosslinked resin is also expected good enough to sustain 100–150 °C because later the fabricated micro-structure may be used as a template to be infiltrated with other functional inorganic materials. Furthermore, the polymerised resins should also have properly mechanical properties. The material should be flexible and tough enough to sustain the deformation of shrinkage. Meanwhile it should be hard enough to maintain the structure shape.

A number of resins have been used for micro-fabrication, some of which have been commercialised. Regarding to the chemical process, only resin SU-8 has a two-step crosslinking procedure. First there is the formation of a strong acid during the exposure process within the focal spots, followed by an acid-initiated, thermally driven epoxy crosslinking during the post-exposure bake step [28]. SU-8 is provided by MicroChem which is originally developed for the microelectronic industry. The product is supplied as a liquid consisting of an epoxy resin, a solvent and a photo-acid generator. The substrate can be coated using a conventional spinner with the film thickness being controlled by the spinning speed and the resin concentration. The sample of pure liquid resin without solvent can also be sandwiched into two coverslips with a thin spacer which determines the thickness of the polymer film. Upon exposure to a light beam, a strong acid is generated which causes the epoxy resin to form a network with a high crosslinking density when it is heated above a critical temperature provided in a post-exposure bake. The unexposed material is then removed with a solvent in the development process. Because it is a two-step procedure, the formation of micro-structures cannot be monitored during fabrication. Therefore the fabrication parameters cannot be adjusted during the exposure process [14,16]. On the other hand, the absence of a liquid-to-solid transition during the light exposure can minimise the local change in the refractive index, thus creating stable recording conditions. It also permits the fabrication of areas behind the already fabricated features to produce self-supporting structures like a spiral-architecture [29].

Other resins can form micro-structures by the single-step curing procedure upon exposure to light. Commercialised resins include SCR500 [10,13] from Japan Synthetic Rubber Company (limited customer), Ormocer from the Fraunhofer Institute for Silicate research [14,18,30], Nopcocure 800 from San Nopco,

Japan [9,11] and NOA63 from Norland Products Inc. [9,12]. All these resins are polymerised through a single-step radical initiated process and contain a PI which cleavages to produce radicals during light exposure. The polymerised resin is confined to the focal spot of a light beam, while the whole fabrication process can be monitored and optimised with adjusting the fabrication parameters. Although polymerisation is a single-step procedure, the light treatment of a sample can be various according to the different requirement of fabrication. Resin such as Nopcocure 800 is pre-exposed to UV light to increase its viscosity [9]. Then the resin is completely solidified by a 2PP process. For rapid fabrication of bulk structures, only the contours have to be irradiated by femtosecond laser pulses. After washing away the non-irradiated, liquid resin, the structure can be exposed to UV-light resulting in solidification of the inner volume [14]. A bulk structure can also be formed through layer-by-layer laser scanning procedure as a standard 3D sterolithography process [15].

Although commercial resins have good performance, the composition of resins is uncertain and unchangeable. Because some fabricated optical devices have special requirements such as high resolution, transparency at certain wavelengths, a high curing speed and a good thermal stability, customer-made resins are also developed in research laboratories. Customer-made resins have some benefit. A resin can be formulated with specific components to adjust the mechanical and surface properties of the resin and different initiators can be chosen to be adapted to the laser wavelength. The concentration of an initiator can be optimised to obtain the best structure, and more efficient initiators can be applied to resin systems. Recently, we have made significant contributions to this area. A PI has been added into resin IPG (Inorganic polymer glass, RPO, Australia) containing polysiloxane chains with acrylate functional groups attached. The resin has enhanced thermal and optical properties compared with commercialised resin, and the possibility to do 3D sterolithgraphy by IPG resin has been demonstrated [15]. Other resin LN1 containing 8 components of different acrylate (Sartomer) has been developed to achieve resolution down to 200 nm with an increased thermal stability [17]. A single-monomer based resin SR348 (also from Sartomer) has also been developed with a simplified preparation procedure without losing the basic performance of LN1 [31].

5.2. Devices

Since 2PP is based on a non-linear interaction of the focused laser pulses with photosensitive resin, it can be used to initialise the polymerisation process anywhere in the volume of the resin and hence allows for the direct fabrication of an arbitrary 3D micro-structure. This has led to the interesting phenomenon that researchers have demonstrated the power of this technique not only by fabricating functional devices such as photonic crystals or other micro-optical elements but also by producing artistic icon-like structures such as a micro-bull [10], a micro-Venus [14], or the Sydney Opera House [15].

In the following the principle steps for the fabrication of 3D micro-structures based on computer generated 3D CAD (computer aided design) models are discussed using the example of a Venus statue [14]. The 3D CAD model can be any kind of 3D models consisting of closed surfaces. In a first step, the model is transformed to a surface model composed of triangles in such a way that all adjacent triangles share two common vertices (see Fig. 7, step A). In a next step, the model has to be sliced, i.e. the intersections of the triangle edges with planes in certain heights have to be calculated resulting in a closed contour for each height (see Fig. 7, step B). The distance between the single slices has to be adapted to the focal length of the laser to provide connected layers. By scanning the laser focus along the contour of each plane and moving the sample in the z-direction in between the planes, the model can be fabricated. The process time to build the Venus statue shown in Fig. 8(A) and (B) and was about 5 min. Only the outer shell was irradiated by fs pulses. The inner volume was solidified using a UV-lamp after the surrounding liquid resin was washed away. Fig. 8(C) and

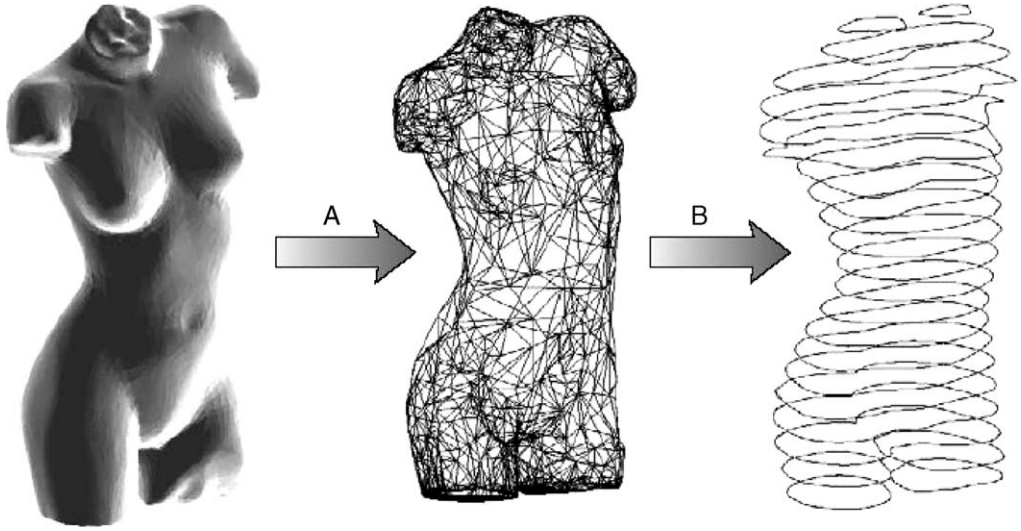

Fig. 7. Images of a computer generated Venus model.

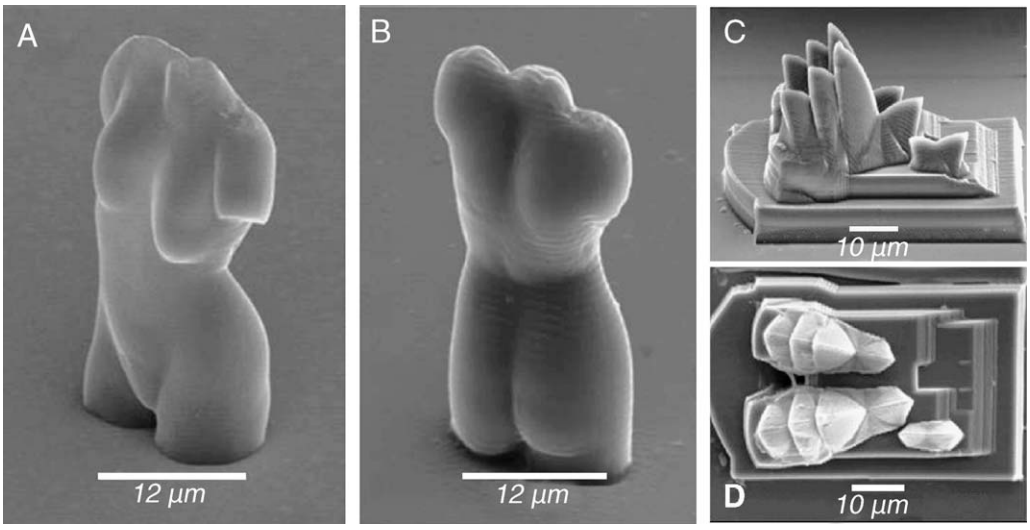

Fig. 8. Images of different micro-models fabricated by means of 2PP. (A) and (B) Venus statue, material: ORMOCER resin; (C) and (D) Sydney Opera House, material: IPG resin.

(D) shows a micro-scale model of the Sydney Opera House that was fabricated by means of 2PP in resin IPG [15]. 2PP technology can also be applied to produce micro-devices such as gear wheels [9] and light driven rotors [12]. Table 2 summaries the common resins used for micro-fabrication, the preparation and post-processing methods, the icon structure of a specific resin and the minimum size of the structure.

The challenge for 2PP technology is to produce isolated or only weekly linked structural elements, in an order of 200 nm, such as woodpile structures for photonic crystal application. A photonic crystal refers to the periodical structure due to the lattice of refractive index contrast at the scale of light wavelength [16]. A photonic crystal can produce bandgaps, which can suppress the light transmission. A 3D photonic crystal has a periodical structure in all three dimensions, and a woodpile structure is the most fabricated 3D photonic crystal structure.

Fig. 9(A) shows a computer generated sketch of a woodpile structure, which is a 3D photonic crystal that can easily be fabricated by means of 2PP. The woodpile structure consists of layers of one-dimensional rods with height h and width w and has a stacking sequence that repeats itself every four layers. The distance between four adjacent layers is denominated by c. Within each layer, the axes of the rods are parallel to each other with a distance δx between them. The adjacent layers are rotated by 90°.

Table 2
Common resins used for two-photon micro-fabrication

Resin	Type of material	Preparation	Post-processing	Icon bulk-like structure	Mini. isolated voxels (nm)
SU-8	Epoxy (2-step reaction)	Use directly (MicroChem)	(1) Post-bake, (2) Washout in special developer	–	–
SCR500	Urethane acrylate	Use directly (Japan Synthetic Rubber Co., limited customers)	Washout in ethanol	Micro-bull [10]	120
Ormocer	Inorganic-organic hybrid	Use directly (Fraunhofer Institute Silicatforschung)	(1) Washout by 4-methyl-2-pentanone, (2) UV pos-curing	Venus torso [14]	120
IPG	Inorganic-organic polysiloxane polymer	PI is added to commercial resin (RPO Inc.)	Washout by toluene	Sydney Opera House [15]	
LN1	Urethane acrylate	8 (Sartomer) components are mixed, (2) PI is added	Washout by ethanol	–	–
SR348	Ethoxylated (2) bisphenol A dimethacrylate	Initiator is added in this resin (Sartomer)	Washout by ethanol	–	–
Nopcocure 800	Acrylic acid ester	(1) Pre-expose UV light to increase viscosity, (2) 2PP process form microstructure	Washout by acetone	Gear wheel [9]	
NOA63	Mercapto-ester polyurethane	Use directly (Norland Products)	Washout by chloroform, acetone	Light driven rotor [12]	

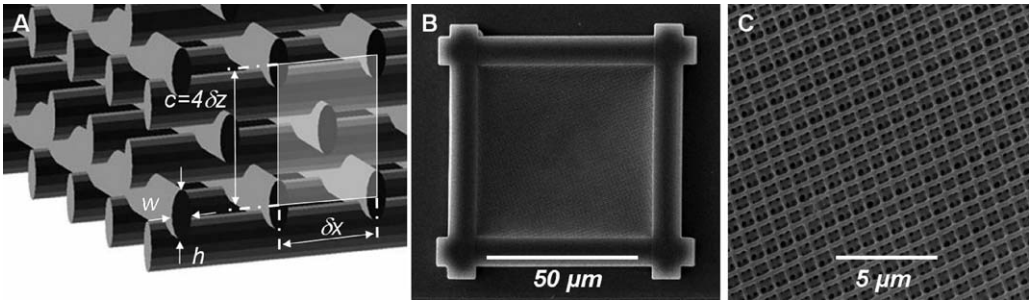

Fig. 9. (A) Computer generated sketch of a woodpile structure. (B) and (C) SEM images of woodpile structures fabricated by means of 2PP. (B) A solid frame was build around the structure to prevent it from shrinking. (C) More detailed view of this woodpile structure. The rods have a width of 200 nm and a periodicity of 800 nm.

Between every other layer, the rods are shifted relative to each other by δz. Generally, the resulting structure has face-centered-tetragonal lattice symmetry. For the special case of $(c/\delta x)^2 = 2$, the lattice can be derived from a face-centered-cubic (fcc) unit cell with the basis of two rods [32]. All of the calculations and experiments shown were performed using fcc lattices.

SEM images of a woodpile structure fabricated in ORMOCERs by the 2PP technique are shown in Fig. 9(B) and (C). The displayed structure consists of rods having a width of 200 nm and an in-layer rod distance of 800 nm. The photonic band structure of the respective photonic lattice was calculated by applying the available software package MPB [33] which is based on the plane-wave-expansion method. The transmission spectrum of the photonic crystal structures was measured by means of Fourier-transform infrared spectroscopy and is shown in Fig. 10. A decrease in transmission of approximately 70% was found at a wavelength of 1.21 μm, which corresponds to a normalized frequency of $\omega = 0.66$ for an in-layer rod spacing of 800 nm. This drop in transmittance corresponds to the fundamental band gap between the 2nd and 3rd bands in the (Γ–X)-direction which is indicated by the shaded area in the band structure [34].

Because telecommunication photonic devices operate at wavelengths of about 1.3–1.55 μm, the bandgap of the photonic crystals should be pushed from long wavelengths to this NIR range. Since the wavelength of the photonic band gap scales with the size of the photonic crystal lattice, a high resolution (i.e. a small size of the rods) is needed to allow for the fabrication of shorter wavelength band gap structures. The rod size of the structure can be reduced by using low laser power. However, it can be limited if the polymerisation reaction spreads into regions beyond the focal spot. In this case, the size of the polymerised volume cannot be further reduced by means of laser power.

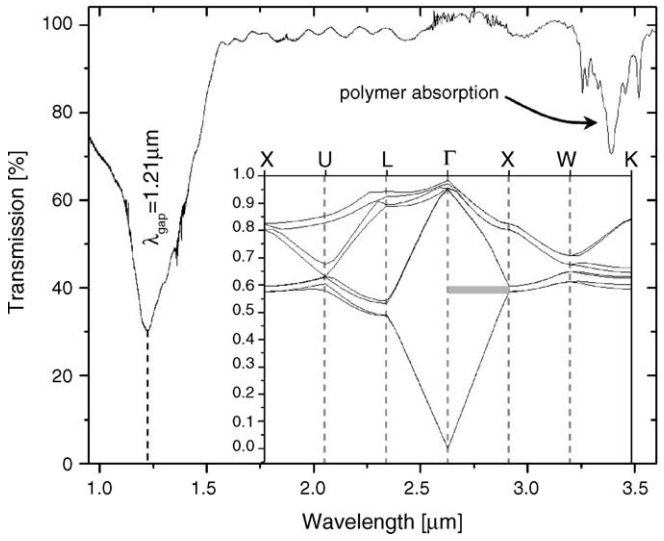

Fig. 10. Measured transmission spectrum of a woodpile structure fabricated by means of 2PP. The inset shows the calculated band structure with a band gap in the (Γ–X)-direction indicated by the shaded area [34].

Furthermore, the resin should have low shrinkage and distortion during polymerisation process, and good mechanical properties to sustain shrinkage and washout processes. The suppression of IR light transmission (%) should be as high as possible. Table 3 summaries the performance of common resins for fabrication of woodpile structure photonic crystals. The structural parameters of woodpile structures, the minimum structural element size (nm), the shortest photonic bandgap wavelength

Table 3
3D Photonic crystals woodpile structures fabricated by common resins

Resin	PCs structure (for shortest wavelength gap one)	Mini. structure size (nm)	Shortest wavelength bandgap (μrn)	Max. suppression of transmission of light (%)
SU-8	Woodpile, $\delta x = 800$ nm, $(c/\delta x)^2 = 2$, 24 layers	180	1.3	72 [16]
SCR500	Woodpile, $\delta x = 1500$ nm, $\delta z = 500$ nm, 40 layers	200	1.5	50 [13]
Ormocer	Woodpile, $\delta x = 700$ nm, $(c/\delta x)^2 = 2$	200	1.2	70 [34]
IPG	Woodpile, $\delta x = 1500$ nm, $\delta z = 1000$ nm, 20 layers	350	4.2	20 [15]
LN1	Woodpile, $\delta x = 1500$ nm, $\delta z = 500$ nm, 40 layers	200	2.3	40 [17]
SR348	Woodpile, $\delta x = 1500$ nm, $\delta z = 500$ nm, 40 layers	300	1.9	39 [31]

(μm), as well as the suppression of IR light transmission (%) are listed in this table as the key performance indicators of the resins. SU-8 has an outstanding performance among all these resins, even through it has complicated fabrication procedure. Ormocer has the shortest wavelength gap. Among the customer-made resins, SR348 has the simplest preparation procedure without losing the basic performance for photonic crystal applications.

Acknowledgements

This work is produced with the assistance of the Australian Research Council under the ARC Centres of Excellence Program. CUDOS (the Centre for Ultrahigh-bandwidth Devices for Optical Systems) is an ARC Centre of Excellence. The authors thank Dr. Dru Morrish for providing Fig. 1.

References

[1] I. Perez-Arjona, G. de Valcarcel, E. Roldan, Revista Mexicana De Fisica 49 (2003) 91.
[2] M. Goeppert-Mayer, Ann. Phys. 9 (1931) 273.
[3] C. Raman, Indian J. Phys. 2 (1928) 387.
[4] W. Kaiser, C. Garret, Phys. Rev. Lett. 7 (1961) 229.
[5] C.M. Blanca, S. Hell, Opt. Express 10 (2002) 893.
[6] D. Morrish, Morphology Dependent Resonance of a Microshere and Its Application in Near-Field Scanning Optical Microscopy, PhD Thesis, Faculty of Engineering and Industrial Science, Swinburne University of Technology, 2005.
[7] N. Rezai, BioTeach J. 1 (2002) 75.
[8] S. Maruo, O. Nakamura, S. Kawata, Opt. Lett. 22 (1997) 132.
[9] H.B. Sun, T. Kawakami, Y. Xu, J.Y. Ye, S. Matuso, H. Misawa, M. Miwa, R. Kaneko, Opt. Lett. 25 (2000) 1110.
[10] S. Kawata, H.B. Sun, T. Tanaka, K. Takada, Nature 412 (2001) 697.
[11] H.B. Sun, S. Matsuo, H. Misawa, Appl. Phys. Lett. 74 (1999) 786.
[12] P. Galajda, P. Ormos, Appl. Phys. Lett. 78 (2001) 249.
[13] M. Straub, M. Gu, Opt. Lett. 27 (2002) 1824.
[14] J. Serbin, A. Ovsianikov, B. Chichkov, Opt. Express 12 (2004) 5221.
[15] M. Straub, L.H. Nguyen, A. Fazlic, M. Gu, Opt. Mater. 27 (2004) 359.
[16] M. Deubel, G. Von Freymann, M. Wegener, S. Pereira, K. Busch, C.M. Soukoulis, Nat. Mater. 3 (2004) 444.
[17] L.H. Nguyen, M. Straub, M. Gu, Adv. Funct. Mater. 15 (2005) 209.
[18] J. Serbin, A. Egbert, A. Ostendorf, B. Chichkov, R. Houbertz, G. Domann, J. Schulz, C. Cronauer, L. Frohlich, M. Popall, Opt. Lett. 28 (2003) 301.
[19] S. Maruo, K. Ikuta, H. Korogi, Appl. Phys. Lett. 82 (2003) 1.
[20] J.M. Kim, H. Muramatsu, Nano Lett. 5 (2005) 309.
[21] Y.V. Miklyaev, D.C. Meisel, M.A. Blanco, G. Von Freymann, K. Busch, W. Koch, C. Enkrich, M. Deubel, M. Wegener, Appl. Phys. Lett. 82 (2003) 1284.
[22] H.F. Grunber, Prog. Polym. Sci. 17 (1992) 953.
[23] K.D. Belfield, X.B. Ren, E.W. Van Stryland, D.J. Hagan, V. Dubikovsky, E.J. Miesak, J. Am. Chem. Soc. 122 (2000) 1217.
[24] M. Rumi, J.E. Ehrlich, A.A. Heikal, J.W. Perry, S. Barlow, Z. Hu, D. McCord-Maughou, T.C. Parker, H. Rockel, S. Thayumanavan, S.R. Marder, D. Beljonne, J.-L. Bredas, J. Am. Chem. Soc. 122 (2000) 9500.
[25] T.C. Lin, S.J. Chung, K.S. Kim, X.P. Wang, G.S. He, J. Swiatkiewicz, H.E. Pudavar, P.N. Prasad, Adv. Polym. Sci. 161 (2003) 157.
[26] W. Zhou, S.M. Kuebler, K.L. Braun, T. Yu, J.K. Cammack, C.K. Ober, J.W. Perry, S.R. Marder, Science 296 (2002) 1106.
[27] B.H. Cumpston, S.P. Ananthavel, S. Barlow, D.L. Dyer, J.E. Ehrlich, L.L. Erskine, A.A. Heikal, S.M. Kuebler, I.-Y.S. Lee, D. McCord-Maughou, J. Qin, H. Rockel, M. Rumi, X.L. Wu, S.R. Marder, J.W. Perry, Nature 398 (1999) 51.
[28] Products information, http://www.microchem.com/products/su_eight.htm.
[29] K.K. Seet, V. Mizeikis, S. Matsuo, S. Juodkazis, H. Misawa, Adv. Mater. 17 (2005) 541.
[30] K.-H. Haas, Adv. Eng. Mater. 2 (2000) 571.
[31] S. Wu, M. Straub, M. Gu, Polymer 46 (2005) 10246.
[32] S.Y. Lin, J.G. Fleming, D.L. Hetherington, B.K. Smith, R. Biswas, K.M. Ho, M.M. Sigalas, W. Zubrzycki, S.R. Kurtz, J. Bur, Nature 394 (1998) 251.
[33] S.G. Johnson, J.D. Joannopoulos, http://ab-initio.mit.edu/mpb (1999).
[34] J. Serbin, M. Gu, Adv. Mater. 18 (2006) 221.